

Original Article

A novel synthesis of stabilized molecularly imprinted polymer for electropolymerization to detect bismethoxycurcumin from curcuminoid

Meyliana Wulandari^{1*}, Nofrizal Nofrizal², and Syed Azhar Syed Sulaiman³¹ *Department of Chemistry, Faculty of Science and Technology,
State Islamic University of Jakarta (UIN Syarif Hidayatullah), Tangerang Selatan, Banten, 15412 Indonesia*² *Research and Development Center, Ministry of Energy and Mineral Resources, Jakarta Selatan, 12230 Indonesia*³ *School of Pharmaceutical Sciences, Universiti Sains Malaysia Minden, Penang, 11800 Malaysia*

Received: 9 July 2022; Revised: 8 November 2022; Accepted: 18 November 2022

Abstract

The purpose of this study is to synthesize a molecularly imprinted polymer (MIP) for use in an electropolymerization approach to separate bisdemethoxycurcumin (BDMC) from curcuminoid. The template molecule used is 3-(4-hydroxyphenyl) propionic acid (HPPA) serving as a water soluble template with a similar molecular structure to BDMC. Pyrrole is used as the functional monomer (FM). The synthesized ultrathin polymer was reproducible and homogeneous, prepared with a gold electrode. An optimization of conditions to remove the template from the ultrathin film was carried out. The analyte rebinding was investigated with Quartz Crystal Microbalance. Fourier Transform Infra-Red characterized the functional groups before and after washing out the template. An electrodeposition of polymers was achieved at -400 Hz of thickness in 1000 s. The rebinding study showed that adsorption capacity of MIP was higher than that of NIP. Regarding selectivity the BDMC had a higher binding affinity to the MIP than to Curcumin (CUR). MIP sensor demonstrated the ability to discriminate target analyte against a very close analog, curcumin, and exhibited good recovery for use in herbal medicine.

Keywords: bisdemethoxycurcumin, electrosynthesis, functional monomer, molecularly imprinted polymer, quartz crystal microbalance

1. Introduction

The rhizome of turmeric (*Curcuma longa*) belongs to the Zingiberaceae family (Karłowicz-Bodalska, Han, Freier, Smoleński, & Bodalska, 2017). It is widely cultivated in the warm and rainy regions of the world, such as China, India, Indonesia, Jamaica, and Peru. Traditional Indian medicine claims the use of its powder against biliary disorders, anorexia, cough, diabetic wounds, hepatic disorder, rheumatism, and sinusitis (Kanase, & Khan, 2018). The natural yellow pigment is isolated from the rhizome of the *Curcuma longa* plant, namely curcumin and its analog

structures, curcuminoids. Commercial curcumin contains curcuminoids: 77% of curcumin, 17% of demethoxycurcumin (DMC), and 3% of Bisdemethoxycurcumin (BDMC) (Huang *et al.*, 1995). It was reported that BDMC from *Curcuma longa* acts as an inhibitor to inactivate human pancreatic α -amylase that is usually a therapeutic target for oral hypoglycemic agents in type-2 diabetes (Ponnusamy, Zinjarde, Bhargava, Rajamohanam, & Ravikumar, 2012). Curcumin is one of the most active members of the phenolic family in anti-invasion and anti-metastasis. It is recommended to prevent a local recurrence of the primary tumor and the spread of tumor cells (Tomeh, Hadianamrei, & Zhao, 2019; Forms, 2022). DMC was found to be the best inhibitor of MCF-7 human breast tumor cells (Sohail *et al.*, 2021). Therefore, based on the current data available, curcuminoids are potentially good drug candidates for developing new inhibitors for controlling starch

*Corresponding author

Email address: meyliana.wulandari@uinjkt.ac.id

digestion and cancer (Li, Xiang, Zhang, An Guo, & Ye, 2010). However, severe side effects may occur at ineffective doses of these new drug candidates. Therefore, the development of methods for separating curcuminoids is essential before they are applied in pharmaceutical preparations or for detection of off-label use in food products (Forms, 2022).

Several separation methods of curcuminoids have been reported, including high-performance thin-layer chromatography (HPTLC) (Kushwaha, Shukla, Dwivedi, & Saxena, 2021) and High-Performance Liquid Chromatography (HPLC) (Fonseca-Santos, Gremião, & Chorilli, 2017). HPLC methods were found to be suitable for the determination of individual curcuminoids. However, HPLC has become outdated due to the lack of a universal detector, being complex to use (Dong, 2020). The development of simple, rapid, and precise multi-analyte detection needs to be explored, to produce inexpensive and better solutions for these products. Nowadays, Molecularly Imprinted Polymers (MIPs) have received much attention because of their advantages. Molecular imprinting is a technique to create specific target analyte binding sites. The imprinted polymers can be prepared by mixing functional monomer (FM), crosslinker, template, and the initiator in a solvent. After removing the template from the rigid polymer network, binding sites complementary in size, shape, and functional groups to the template molecule can be obtained (Hasanah, Safitri, Zulfa, Neli, & Rahayu, 2021). MIPs are synthetic sorbents designed to retain the target molecule selectively regardless of the complexity of the matrix (Malik, Shaikh, Mustafa, & Bhangar, 2019). They have many advantages such as stability, ease of preparation, low cost, reusability, and resistance to extreme pH and temperature. MIPs are of interest in various applications because of their high stability (Liu *et al.*, 2019). The separation and determination of curcuminoids has been studied by molecular imprinting of composite membranes of poly (methacrylamide-co-methacrylic acid). The composite membrane was synthesized by radical copolymerization using filter paper as a supporting membrane (Thongchai & Fukngoen, 2018). Another way to separate curcuminoids is by using the bulk polymerization method for synthesizing MIPs and then detecting with HPLC (Wulandari, Urraca, Descalzo, Amran, & Moreno-Bondi, 2015).

In recent years, interest has been increasing in electropolymerization as a new strategy in MIPs generation. The development of MIPs based electrochemical sensors constitutes an alternative for the target analyte's rapid, sensitive, and selective determination. The amount of density current during electrodeposition varies in producing a certain thickness (Cui, Liu, Liu, Liu, & Zhang, 2020; Emilsson *et al.*, 2017; Lowdon *et al.*, 2020; Mahapatro & Kumar Suggu, 2018;). Recently, Quartz Crystal Microbalance (QCM) has been used with electrochemistry to investigate polymer formation (Diltemiz, Keçili, Ersöz, & Say, 2017). Since the earliest QCM was reported in 1983, this device has been widely used for biological and clinical diagnoses. The main advantage is the minimal user input required. Based on such findings QCM has become more appropriate for sensing applications (El-Sharif, Aizawa, & Reddy, 2015). QCM is a powerful tool to quantify various modified substances on an electrode and to monitor *in situ* the modification processes (Su *et al.*, 2008). The merits of the QCM are to shorten the assay

time and eliminate expensive lab equipment (Della Ventura, Mauro, Battaglia, & Velotta, 2021). Because of high mass sensitivity and durability, QCM is commonly used to characterize thin layers, fluids, and gases (Syritski, Reut, Opik, & Idla, 1999).

Therefore, electropolymerization was studied to separate BDMC from curcuminoid, and the template molecule used in this study was 3-(4-hydroxyphenyl) propionic acid (HPPA). HPPA was chosen due to being a water-soluble template with a similar molecular structure to BDMC. HPPA can be used for polymer film deposition from aqueous solutions (Ata & Zhitomirsky, 2012; Hidaka, Kojima, Nakahata, & Sakai, 2021). The functional monomers (FM) used in this study are pyrrole and dopamine, expected to generate homogenous polymers. The synthesized ultrathin polymer was reproducible and homogeneous with a gold electrode. An optimization of conditions to remove the template from the ultrathin film was carried out, and then the analyte rebinding with QCM was tested.

2. Materials and Methods

2.1 Materials

All chemicals used in this work were brought from Sigma Aldrich (Darmstadt, Germany) with >99% purity, bisdemethoxycurcumin (BDMC), curcumin (CUR), 3-(4-hydroxyphenyl) propionic acid (HPPA); and with 98% purity pyrrole, dopamine, phosphate-buffered saline (PBS), sulfuric acid, 30% hydrogen peroxide, sodium hydroxide (NaOH), milliQ and distilled water. Phosphate buffer saline (PBS, pH 7) was prepared by mixing 39 ml of 0.1 M sodium phosphate monobasic and 61 ml of 0.1 M sodium phosphate dibasic solution and brought to a final volume of 200 ml with deionized water.

2.2 Prepolymerization study (monomer selection)

UV-vis spectroscopic studies on the prepolymerization complex were performed to select the proper FM to form noncovalent bonds with template molecules. Pyrrole and dopamine were studied in an aqueous solution. The concentration of the template molecule was kept constant and gradually the concentration of the monomer was increased. We used UV-vis measurement to evaluate the interaction between the template molecule and each selected monomer. The focus was on complex formation between the monomer and the template molecule: when there is a shift change on increasing the monomer concentration relative to the template. HPPA as a template soluble in water was prepared. About 1.5 mL HPPA ($5.15 \cdot 10^{-4}$ M) was titrated with pyrrole ($1 \cdot 10^{-4}$ M) and dopamine ($7.49 \cdot 10^{-5}$ M) with additional volume of 1, 10, 20, 50, 100, 200, 500, 1000, 1500, 2000, or 2500 μ L was added.

2.3 Pretreatment of the working electrode (WE)

A gold electrode (od: 2 mm and 8 mm) with 1.37 cm^2 area exposure and equipped with a 5 MHz quartz crystal microbalance (QCM) sensor (Maxtek, Inc.) was used as the working electrode for electrodeposition. Reference and counter electrodes were RE: Ag/AgCl in sat KCl and CE: Pt

wire, respectively. The working electrode was subjected to the following cleaning procedure before use. In chemical pretreatment the electrode was dipped into H₂O₂: H₂SO₄ =1:3 v/v solution for 10 min to remove all the organic residues. Then the electrode was rinsed with water and dried by nitrogen. Before the electropolymerization of pyrrole, the gold electrode (QCM) was treated electrochemically in 0.1 M H₂SO₄ aqueous solution by cycling the electrode potential in the range -0.2 – 1.5 V (scan rate 50 mV/s) until cyclic voltammograms were reproducible. Finally, the electrodes were rinsed with distilled water.

2.4 Determination of oxidation potential of monomer dopamine and pyrrole in aqueous solution

Electrochemical polymerization of monomers has been studied by cyclic voltammetry. It was carried out in a 2 mL Teflon electrochemical cell connected with reference 600 Potentiostat (Gamry Instrument, USA). The electrode used was to determine the oxidation potential of the template molecule as described above. The concentrations of dopamine and pyrrole were 0.1 M and 0.1 M.

2.5 Study of electropolymerization of the selected monomers in the presence of template molecule

NIP and MIP thin films were electrodeposited on the QCM sensor at a potential of 0.6V vs. Ag/AgCl/KCl sat in PBS solution and 0.1 M pyrrole (NIP) and 0.1 M pyrrole and 0.1 M HPPA (MIP). Comparison of the ratio of monomer and template with a ratio of 1. To obtain a similar thickness of NIP (pyrrole) and MIP (pyrrole + HPPA), the electrochemical quartz crystal microbalance (EQCM) method was applied. EQCM measurements were performed with a QCM100 system (Stanford Research Systems, Inc., Sunnyvale, CA, USA) coupled to a potentiostat (Gamry Instruments, Inc.).

The synthesis of NIP and MIP was carried out at a resonant frequency down to -400 Hz when the deposited polymer had to look uniform. The film thickness was estimated by converting the frequency shift to the corresponding mass using Sauerbrey's equation (Equation 1) and dividing by the polymer density (Equation 2). After the synthesis of MIP and NIP, the EQCM working electrode was washed with water and dried under nitrogen flow.

$$\Delta f = -f_0^2 \Delta m / N \rho_q = -C_f \Delta m \quad (1)$$

$$t_f = \Delta m / \rho_f \quad (2)$$

where f: resonant frequency shift (Hz), f₀: fundamental frequency of the crystal (Hz), m: mass change (g/cm²), N: frequency constant for quartz (167 kHz cm), ρ_q: density of quartz (2.65 g/cm³), C_f: sensitivity factor (for 5 MHz quartz crystal, 56.6 Hz mg⁻¹ cm²), t_f: the thickness of the film, and Δf: density of the film (Ayankojo, Reut, Ciocan, Öpik, & Syrtiski, 2020).

2.6 Washing procedure

To achieve good sensitivity and reproducibility of

MIP, the template removing treatment needs to be improved because more imprint sites can ensure a better analytical performance. The reaction mechanism used sodium hydroxide (0.1 N) as hydrolysis solvent. The results indicated that alkali-based hydrolysis removes the template faster. In this work, NaOH solution was used to wash out the template molecule with stirring for 24 hours. The polymer was not soluble in water, but the template molecule was soluble. Therefore, NaOH 0.1 N was used as a washing solution. After that, the gold slide consists of polypyrrole (PPy) with template HPPA before removing (a) and after removing the template molecule (b) compared with the polymer that polymerized without template (c) were studied by FT-IR.

2.7 QCM Rebinding study

The QCM technique on the MIP-HPPA was used to study the rebinding of the HPPA as a target molecule. This technique enables the investigating of molecular interactions in the QCM area. The QCM was connected to an injector pump (Cavro XLP 6000® XLP 6000, Tecan Nordic AB, Mölndal, Sweden), a motorized six-way port injection valve (C22-3186EH, VICI® Valco Instruments Company Inc., USA) controlled by a microelectronic actuator and a small volume (150 μL) axial flow cell attached to the QCM sensor holder (Stanford Research Systems, Inc.). Samples were injected with a 5 mL disposable plastic syringe. All QCM systems are connected to a PC and controlled by Labview Software. PBS buffer flowed continuously at a flow rate of 25 μL/min to obtain a continuous baseline. Afterward, a series of HPPA concentrations (1.25 x 10⁻⁴, 2.5 x 10⁻⁴, 5 x 10⁻⁴, 1 x 10⁻³, 1.5 x 10⁻³, 2 x 10⁻³ M of the HPPA in PBS buffer) was injected at a 50 μL/min flow rate to an injection loop (500 μL). The experiments were repeated three times (n=3). Before the rebinding study, the HPPA MIP films and their NIP as references were regenerated by immersing the QCM sensor modified films in sodium hydroxide (0.1 N) solution for 24 h.

3. Results and Discussion

3.1 Pre-polymerization study

UV-vis absorption spectra of the template and FM were recorded in a 1 cm quartz cuvette (Shimadzu 2401 spectrophotometer) in the wavelength range from 200 to 300 nm. This study aims to obtain an FM complementary to the template and stabilize and maximize the complex formation. It will be time-consuming to search FM by using some monomers in polymerization then measuring its binding affinity to recognize template molecules. This pre-polymerization study using spectroscopic method was initiated due to it being a rapid and valuable tool to evaluate the FM's interaction and template solution (chemical structures can be seen in Figure 1).

Figure 2a shows the titration of HPPA (5.10⁻⁴ M) by dopamine (7.49.10⁻⁵ M) in an aqueous solution. The higher the concentration of HPPA reacted with dopamine, the higher the absorbance produced. The redshift (a change in absorbance to a larger wavelength) is observed for absorption band at about 280 nm, being strong evidence of complex formation between the two compounds. Figure 2b shows the changes in the HPPA adsorption band at 230 nm upon adding pyrrole at

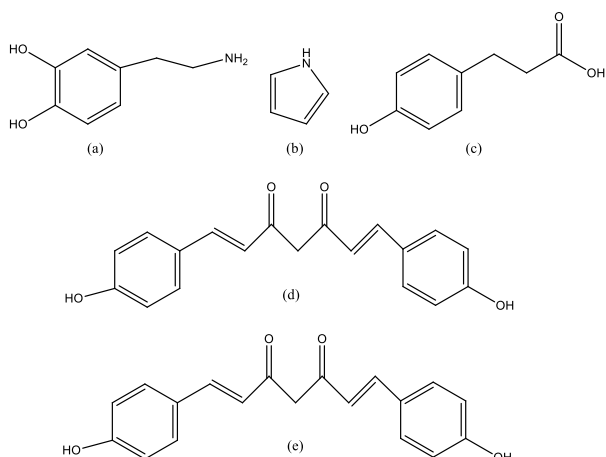


Figure 1. Chemical structures of dopamine (a), pyrrole (b), HPPA (c), BDMC (d), and CUR (e) that were included in this study.

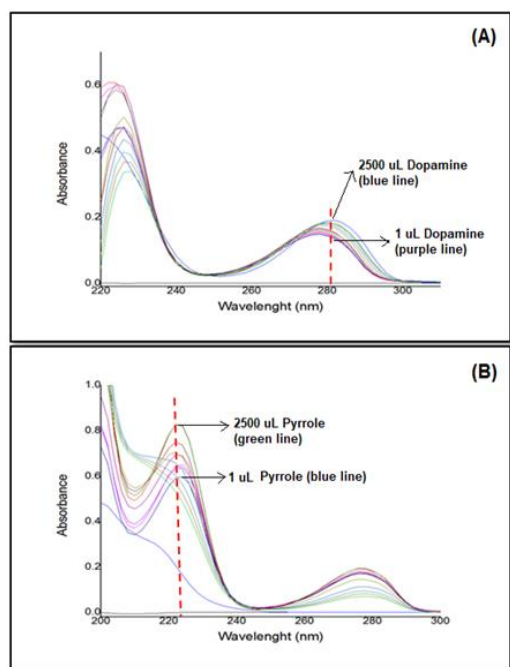


Figure 2. Spectroscopic evaluation of the pre-polymerization complex formation between HPPA ($5.15 \cdot 10^{-4}$ M) and dopamine ($7.49 \cdot 10^{-5}$ M) in water (a); HPPA ($5.15 \cdot 10^{-4}$ M), and pyrrole ($1 \cdot 10^{-4}$ M) in water (b).

concentrations $1 \cdot 10^{-4}$ M, indicating possible interactions between pyrrole and HPPA in water. This can be evidence of complex formation between HPPA and pyrrole in an aqueous solution. Such a complex leads to the formation of well-defined specific binding sites in the imprinted polymer.

3.2. Study of the electrochemical polymerization to generate homogeneous polymer film

The electrochemical polymerization of the selected monomers in the presence of template molecule HPPA was studied to find optimal synthesis parameters and prepare

homogeneous and stable polymer film on the electrode. The experimental data are summarized in Table 1.

The experiment setup for electrochemical quartz crystal microbalance (EQCM) is shown in Figure 3. The voltammograms of dopamine and pyrrole electrochemical oxidation in the presence of HPPA in an aqueous PBS solution are presented in Figure 4. In Figure 4a, it can be seen that dopamine electrochemical oxidation is significantly suppressed in the presence of HPPA: no oxidation peak can be observed; therefore, polymerization was unsuccessful in an aqueous solution with 0.1 M HPPA at $E_{app} = 0.6$ V. This might be because dopamine doesn't have a rich electron heterocyclic group.

Meanwhile, when pyrrole was used as a monomer, homogeneous MIP films were obtained in an aqueous solution containing 0.1 M pyrrole and 0.1 M HPPA at $E_{app} = 0.6$ V in potentiodynamic mode. The presence of HPPA in the mixture slowed down the electrochemical oxidation process: the oxidation potential was shifted by ca. 300 mV to be more anodic with a simultaneous decrease of anodic current (Figure 4b). However, the polymerization process can still proceed, leading to a homogeneous polymer film on the electrode surface. Based on the presented voltammograms, the polymerization potential of the corresponding monomer in the presence of HPPA can be used to prepare thin polymer film on the sensor surfaces of QCM.

Table 1. Film formation

Monomer	Template	Result
Dopamine (0.1 M)	HPPA (0.1 M)	No film formed
Pyrrole (0.1 M)	HPPA (0.1 M)	Homogeneous film formed

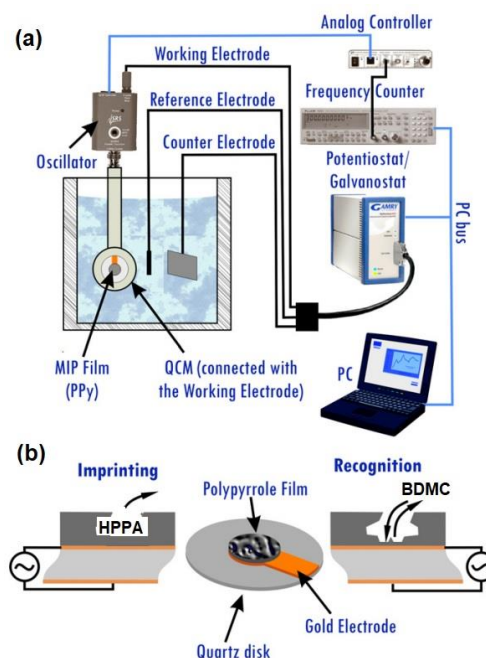


Figure 3. Electrochemical Quartz Crystal Microbalance (EQCM) setup (a), the polypyrrole film and the recognition of BDMC as a target molecule (b)

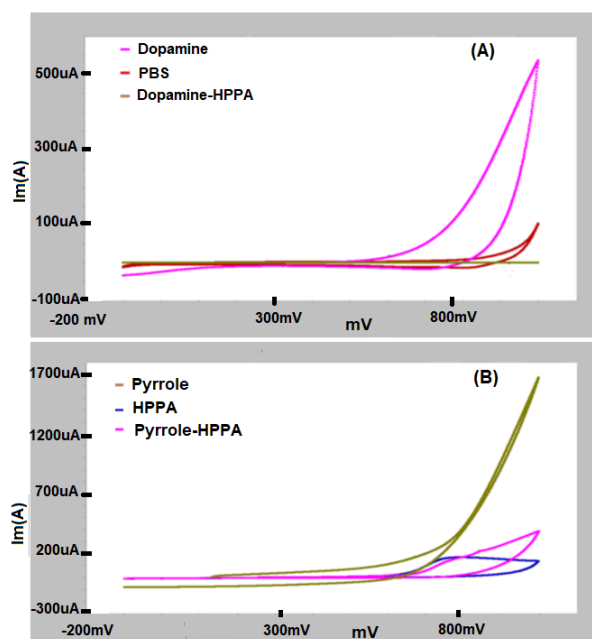


Figure 4. Cyclic voltammograms of 0.1 M dopamine and 0.1 M HPPA (a), and 0.1 M pyrrole and 0.1 M HPPA (b) in an aqueous solution

3.3. Polymerization on QCM and molecule template extraction

Figure 5 shows typical resonance frequency responses of the QCM during the potentiostat electrodeposition. The film growth rate of the MIP in the presence of the template was much slower than the rate for the NIP film at the same polymerization conditions. The monomer used can be polymerized into polypyrrole (PPy) (Figure 5a). This polymer is conductive, causing a fast polymerization rate (Yussuf, Al-Saleh, Al-Enezi, & Abraham, 2018). Thin films of PPy, electropolymerized in the presence of HPPA as template molecules to create complementary-shaped cavities, were evaluated as MIPs. The films were formed on gold-coated quartz crystals, and the EQCM technique determined frequency changes of the polymeric films during electropolymerization.

When a non-conductive template is involved in polymerization, the polymerization rate slows. Then, to achieve the same film thicknesses for MIP and NIP, the MIP required a longer polymerization time. As observed in Figure 5, the MIP films grew linearly, followed by their gradual slowing-down until the resonant frequency drop of -400 Hz in 1000 s. For NIP the frequency drop was achieved in 330 s. This result was comparable to previous research to detect Amoxicillin compounds with the QCM method. In this study, using similar polymer thickness (-400 Hz), the deposition times needed for MIP and NIP are 900 and 200 seconds, respectively (Yang, Hong, & Park, 2021).

Figure 6a shows that when pyrrole polymerizes to polypyrrole (PPy) (Tan & Ghandi, 2013), then poly-pyrrole reacts with an HPPA template molecule, and an amide is formed. This is evidenced by the infra-red spectrum in the 1600-1800 cm^{-1} region which indicates an absorption band of

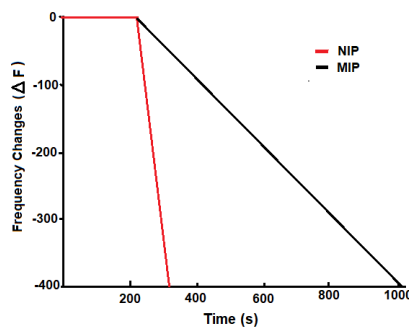


Figure 5. Resonant frequency responses during the potentiostat electrodeposition of Py/MIP and NIP on the gold electrode of QCM. WE: Au(QCM), RE: Ag/AgCl/KCl(sat), CE: Pt, Template: 0.1 M HPPA, FM: 0.1 M Py, V: 0.6 V.

the amide group. After polymerization was carried out, template molecule extraction was required to produce particular sites for the target molecule. In this study, as shown by Figure 6b, the extraction of template molecules was carried out by hydrolysis of the amide in a dilute alkaline environment. The hydrolysis of amides can be carried out with dilute strong acids or bases (Fendler, Fuller, Perry, & Rocek, 1965). Using strong bases to extract template molecules will not damage the polymer structure at the active site that has been formed. The selective active site for BDMC will be used for rebinding studies, while the template molecule that has been extracted will not be used again in the study. Characterization of the success of the washing-out procedure was carried out by Fourier Transform Infra-Red Spectrophotometer (IR Prestige-21 Fourier Transform Infrared Spectrophotometer Shimadzu). From Figure 7, when the template molecule was extracted, no amide group appeared.

3.4. Rebinding study

After forming a selective cavity for the HPPA template molecule, then HPPA rebinding analysis is carried out using the QCM technique. NIP as a control polymer is essential to provide good rebinding analysis results to compare with the MIP. Rebinding experiments were carried out in a closed custom-designed insulating chamber. The concentrations of HPPA as an analyte were set at 1.25×10^{-4} , 2.5×10^{-4} , 5×10^{-4} , 1×10^{-3} , 1.5×10^{-3} , and 2×10^{-3} M, see the plot in Figure 8. For the NIP, when the concentration of HPPA increased from 1.25×10^{-4} M to 5×10^{-4} M, there was an increase in frequency changes, which then reached equilibrium and saturated. For MIP-HPPA, as the concentration increased, the adsorption of MIP also increased. MIP has higher adsorption compared to NIP. The data indicate that we could recognize HPPA with MIP film. The imprinting sites of MIP were filled with the analyte molecules. NIP also has negligible adsorption; it was physical adsorption on the surface of film. This study is supported by previous research using a concentration of amoxicillin in the range 0-1000 M, resulting in frequency resonance changes for MIP greater than for NIP (Yang *et al.*, 2021).

Polymer thickness was studied to determine its effect on the adsorption process of the target molecule. The thickness of the polymer obtained from the resonant frequency

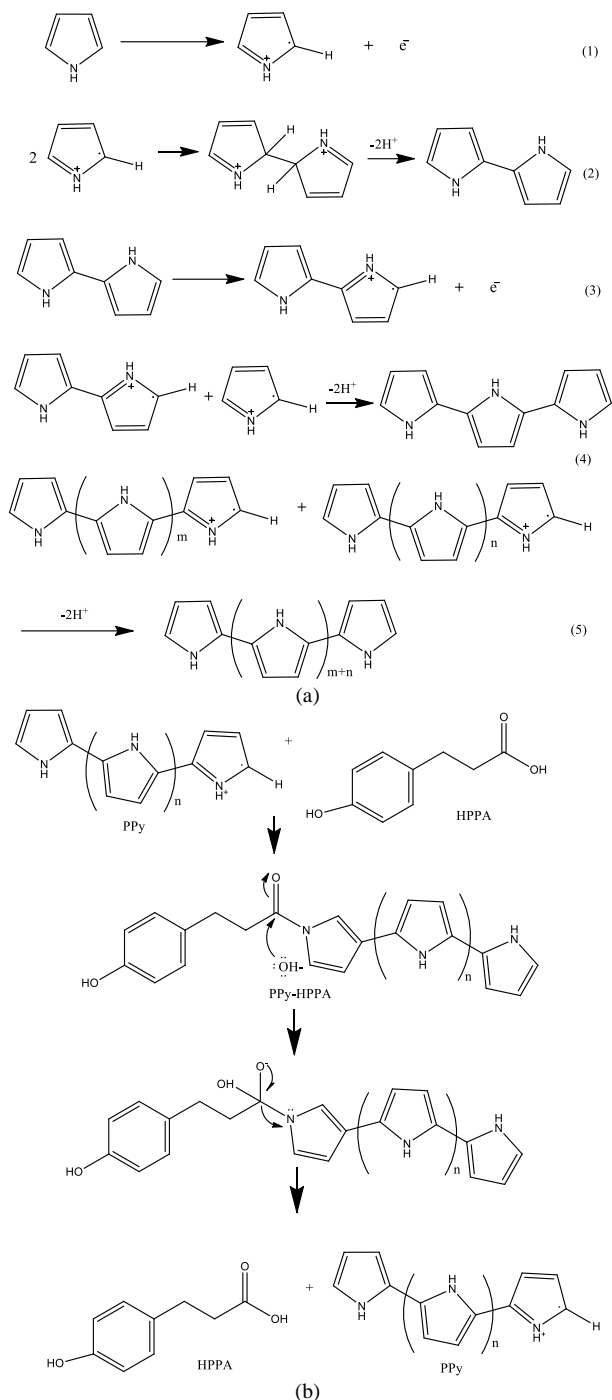


Figure 6. Polymerisation of pyrrole (a), possible reaction mechanism between pyrrole and HPPA and hydrolysis reaction in washing out procedure (b)

changes in the electrodeposition of the polymer (i.e., 100, 250, and 400 Hz, respectively) being equal to 6.3, 15.6, and 25.0 nm (Equation 1 and 2). The injection of 1 mM concentration of HPPA resulted in the data in Figure 9. When the polymer thickness increases, the specific surface area will increase the number of binding sites in MIP-HPPA. It can be seen in the figure that the thicker the polymer, the higher the imprinting

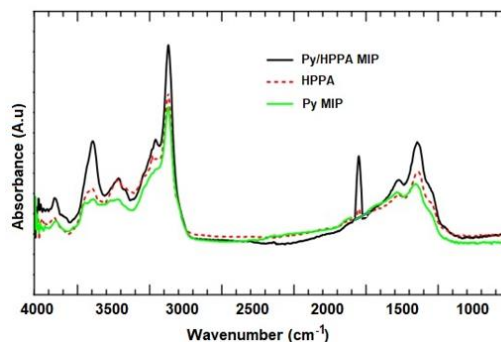


Figure 7. Infra-red spectrophotometry of template HPPA, Py/HPPA MIP, and Py MIP after washing

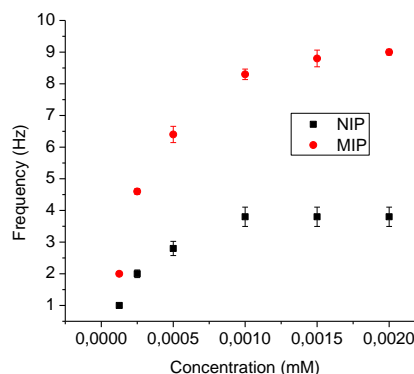


Figure 8. Rebinding study of HPPA on PPy-MIP film in PBS, flow rate 50 uL/min, 500 uL volume of the loop, a polymer consisting of poly-py -400 Hz (25 nm)

factor/IF (changes the resonant frequency of MIP/NIP) so that the adsorption increases. The IF for the thicknesses of 6.3, 15.6, and 25.0 nm were 1.3, 2.5, 2.6. These results are consistent with previous studies, which concluded that the growing polymer would increase the IF (Kidakova *et al.*, 2020; Yang *et al.*, 2021).

The environment presents a blend of different molecules and compounds. Thus, an environmental sample for BDMC detection may contain other molecules different from the target. These interfering molecules can affect the performance of a MIP sensor through cross-reactivity with the MIP binding sites. Consequently, one of the factors determining the quality of a MIP sensor is its selectivity, i.e., the ability to show preferential binding towards the target in the presence of other similar or interfering molecules. The selectivity of MIP-HPPA was tested using samples containing structures similar to BDMC. To study the selectivity of the prepared MIP-HPPA, BDMC and curcumin (as other curcuminoids) were selected.

The individual selectivity for BDMC of the imprinted PPy films was determined under the conditions of PBS containing 1; 1.5; 2 mM of BDMC and curcumin at a flow rate of 12.5 uL/min with an injection loop of 250 uL size. The frequency response was monitored in a buffer solution until a constant baseline signal was reached followed by the injection of the sample containing one of the curcumins. The frequency change was monitored until the steady state was reached. Figure 10 describes the ratio of the

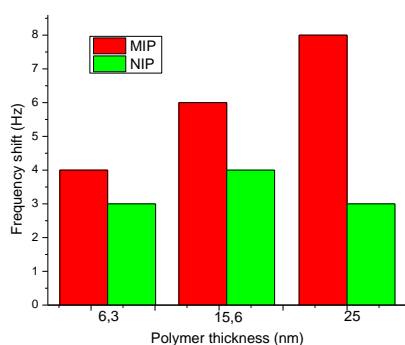


Figure 9. Effect of the thickness of synthesized polymer on the Imprinting Factor (IF)

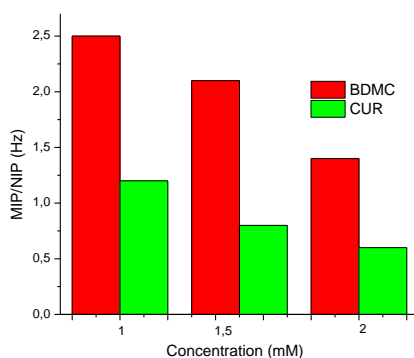


Figure 10. Resonance frequency response of MIP/NIP upon injection of BDMC and CUR

equilibrium binding response of each analyte on the MIP-HPPA to that on the NIP. It can be seen that as the concentration of target molecules (BDMC) increases resonant frequency changes become lower. As expected, the imprinted surface had more significant relative adsorption of the BDMC target molecules. In contrast, the adsorption of the non-target curcuminoid (curcumin) was considerably lower. This is probably due to the HPPA template molecules for MIP being imprinted, preferring to bind to BDMC more than to curcumin. Curcumin has a methoxy group which acts as a steric barrier for it to attach to the active site of MIP.

Furthermore, to validate the sensor's accuracy and practical application, recovery experiments were carried out using herbal medicine samples spiked with different concentrations of BDMC (Table 2). Percentage recovery was calculated by finding the difference between measured BDMC concentration in spiked and non-spiked samples and dividing by the amount spiked. It can be observed that MIP demonstrates good recovery, with the value ranging between 91% and 104%, validating its accuracy and practical suitability.

4. Conclusions

This work demonstrated the electrosynthesis of MIP-HPPA prepared by the QCM technique. HPPA as the mimic molecule was the best choice to produce specific binding capacity for the target molecule because of being water-soluble. The polymerization of pyrrole with template molecule HPPA and the absence of HPPA provide

homogeneous and stable polymer film on the electrode surface. The template removal procedure was successfully done by hydrolysis in alkaline conditions. The rebinding of the template was tested. Study showed that the MIP has a higher adsorptive capacity than NIP. When the polymer thickness increases, it is followed by an increase in IF. Furthermore, the sensor shows good recoveries, ranging from 91 to 104% in herbal medicine, thereby validating practical applicability in the intended media. Thus, the presented electrochemical approach displays potential for a portable and cost-effective sensor detecting BDMC.

Acknowledgements

The study was conducted in collaboration between two government institutions, namely the Ministry of Energy and Mineral Resources, with State Islamic University (UIN) Syarif Hidayatullah Jakarta. The authors would like to extend their gratitude towards Ministry of Energy and Mineral Resources for the support and facilities utilized in this research.

References

- Ayankojo, A. G., Reut, J., Ciocan, V., Öpik, A., & Syritski, V. (2020). Molecularly imprinted polymer-based sensor for electrochemical detection of erythromycin. *Talanta*, 209(October), 120502. Retrieved from <https://doi.org/10.1016/j.talanta.2019.120502>
- Della Ventura, B., Mauro, M., Battaglia, R., & Velotta, R. (2021). Quartz Crystal Microbalance Sensors: New Tools for the Assessment of Organic Threats to the Quality of Water. *Handbook of Environmental Chemistry*, 102, 315–342. Retrieved from https://doi.org/10.1007/978_2019_390
- Diltemiz, S. E., Keçili, R., Ersöz, A., & Say, R. (2017). Molecular imprinting technology in Quartz Crystal Microbalance (QCM) sensors. *Sensors (Switzerland)*, 17(3). Retrieved from <https://doi.org/10.3390/s17030454>
- Dong, M. W. (2020). Perspectives in Modern HPLC. *Lc Gc North America*, 31(6), 472–479.
- El-Sharif, H. F., Aizawa, H., & Reddy, S. M. (2015). Spectroscopic and quartz crystal microbalance (QCM) characterisation of protein-based MIPs. *Sensors and Actuators, B: Chemical*, 206, 239–245. Retrieved from <https://doi.org/10.1016/j.snb.2014.09.053>
- Fendler, J. H., Fuller, N. A., Perry, S., & Rocek, J. (1965). *The hydrolysis of phosphate diesters with barium hydroxide I.* (6174), 6174–6180.
- Fonseca-Santos, B., Gremião, M. P. D., & Chorilli, M. (2017). A simple reversed phase high-performance liquid chromatography (HPLC) method for determination of in situ gelling curcumin-loaded liquid crystals in vitro performance tests. *Arabian Journal of Chemistry*, 10(7), 1029–1037. Retrieved from <https://doi.org/10.1016/j.arabj.2016.01.014>
- Forms, P. (2022). Curcumin: Biological activities and modern. *Antibiotics*, 11, 1–27.

- Hasanah, A. N., Safitri, N., Zulfa, A., Neli, N., & Rahayu, D. (2021). Factors affecting preparation of molecularly imprinted polymer and methods on finding template-monomer interaction as the key of selective properties of the materials. *Molecules*, 26(18). Retrieved from <https://doi.org/10.3390/molecules26185612>
- Huang, M. T., Ma, W., Lu, Y. P., Chang, R. L., Fisher, C., Manchand, P. S., . . . You, M. (1995). Effects of curcumin, demethoxycurcumin, bisdemethoxy curcumin and tetrahydrocurcumin on 12-O-tetradecanoylphorbol-13-acetate-induced tumor promotion. *Carcinogenesis*, 16(10), 2493–2497. Retrieved from <https://doi.org/10.1093/carcin/16.10.2493>
- Kanase, V., & Khan, F. (2018). An overview of medicinal value of curcuma species. *Asian Journal of Pharmaceutical and Clinical Research*, 11(12), 40–45. Retrieved from <https://doi.org/10.22159/ajpcr.2018.v11i12.28145>
- Karłowicz-Bodalska, K., Han, S., Freier, J., Smoleński, M., & Bodalska, A. (2017). Curcuma longa as medicinal herb in the treatment of diabetic complications. *Acta Poloniae Pharmaceutica - Drug Research*, 74(2), 605–610.
- Kushwaha, P., Shukla, B., Dwivedi, J., & Saxena, S. (2021). Validated high-performance thin-layer chromatographic analysis of curcumin in the methanolic fraction of Curcuma longa L. rhizomes. *Future Journal of Pharmaceutical Sciences*, 7(1). Retrieved from <https://doi.org/10.1186/s43094-021-00330-3>
- Li, R., Xiang, C., Zhang, X., An Guo, D., & Ye, M. (2010). Chemical Analysis of the Chinese Herbal Medicine Turmeric (*Curcuma longa* L.). *Current Pharmaceutical Analysis*, 6(4), 256–268. Retrieved from <https://doi.org/10.2174/157341210793292356>
- Liu, G., Huang, X., Li, L., Xu, X., Zhang, Y., Lv, J., & Xu, D. (2019). Recent advances and perspectives of molecularly imprinted polymer-based fluorescent sensors in food and environment analysis. *Nanomaterials*, 9(7). Retrieved from <https://doi.org/10.3390/nano9071030>
- Malik, M. I., Shaikh, H., Mustafa, G., & Bhangar, M. I. (2019). Recent applications of molecularly imprinted polymers in analytical chemistry. *Separation and Purification Reviews*, 48(3), 179–219. Retrieved from <https://doi.org/10.1080/15422119.2018.1457541>
- Ponnusamy, S., Zinjarde, S., Bhargava, S., Rajamohanam, P. R., & Ravikumar, A. (2012). Discovering bisdemethoxycurcumin from curcuma longa rhizome as a potent small molecule inhibitor of human pancreatic α -amylase, a target for type-2 diabetes. *Food Chemistry*, 135(4), 2638–2642. Retrieved from <https://doi.org/10.1016/j.foodchem.2012.06.110>
- Sohail, M., Guo, W., Yang, X., Li, Z., Li, Y., Xu, H., & Zhao, F. (2021). A promising anticancer agent dimethoxycurcumin: aspects of pharmacokinetics, efficacy, mechanism, and nanof ormulation for drug delivery. *Frontiers in Pharmacology*, 12(July), 1–14. Retrieved from <https://doi.org/10.3389/fphar.2021.665387>
- Su, Y., Xie, Q., Chen, C., Zhang, Q., Ma, M., & Yao, S. (2008). Electrochemical quartz crystal microbalance studies on enzymatic specific activity and direct electrochemistry of immobilized glucose oxidase in the presence of sodium dodecyl benzene sulfonate and multiwalled carbon nanotubes. *Biotechnology Progress*, 24(1), 262–272. Retrieved from <https://doi.org/10.1021/bp070256+>
- Syritski, V., Reut, J., Opik, A., & Idla, K. (1999). Environmental QCM sensors coated with polypyrrole. *Synthetic Metals*, 102(1–3), 1326–1327. Retrieved from [https://doi.org/10.1016/S0379-6779\(98\)01047-9](https://doi.org/10.1016/S0379-6779(98)01047-9)
- Tan, Y., & Ghandi, K. (2013). Kinetics and mechanism of pyrrole chemical polymerization. *Synthetic Metals*, 175, 183–191. Retrieved from <https://doi.org/10.1016/j.synthmet.2013.05.014>
- Thongchai, W., & Fukngoen, P. (2018). Synthesis of curcuminoid-imprinted polymers applied to the solid-phase extraction of curcuminoids from turmeric samples. *Journal of Pharmaceutical Analysis*, 8(1), 60–68. Retrieved from <https://doi.org/10.1016/j.jpha.2017.09.003>
- Wulandari, M., Urraca, J. L., Descalzo, A. B., Amran, M. B., & Moreno-Bondi, M. C. (2015). Molecularly imprinted polymers for cleanup and selective extraction of curcuminoids in medicinal herbal extracts. *Analytical and Bioanalytical Chemistry*, 407(3), 803–812. Retrieved from <https://doi.org/10.1007/s00216-014-8011-5>
- Yang, J. C., Hong, S. W., & Park, J. (2021). Improving surface imprinting effect by reducing nonspecific adsorption on non-imprinted polymer films for 2,4-D Herbicide Sensors. *Chemosensors*, 9(3), 43. Retrieved from <https://doi.org/10.3390/chemosensors9030043>
- Yussuf, A., Al-Saleh, M., Al-Enezi, S., & Abraham, G. (2018). Synthesis and characterization of conductive polypyrrole: The influence of the oxidants and monomer on the electrical, thermal, and morphological properties. *International Journal of Polymer Science*, 2018. Retrieved from <https://doi.org/10.1155/2018/4191747>